Human Molecular Genetics, 2003, Vol. 12, No. 20 **2609–2623**
DOI: 10.1093/hmg/ddg293

Involvement of the ubiquitin-proteasome pathway and molecular chaperones in oculopharyngeal muscular dystrophy

Aida Abu-Baker[1], Christiane Messaed[1], Janet Laganiere[1], Claudia Gaspar[1], Bernard Brais[2] and Guy A. Rouleau[1,*]

[1]Center for Research in Neuroscience, McGill University, and the McGill University Health Center, 1650 Cedar Avenue, Montreal, Quebec H3G 1A4, Canada and [2]Centre de recherché du CHUM, Hopital Notre-Dame, Universite de Montreal, 1560 Sherbrook East, Montreal, Quebec H2L 4M1, Canada

Received May 23, 2003; Revised August 5, 2003 and Accepted August 16, 2003

Oculopharyngeal muscular dystrophy (OPMD) is a late-onset autosomal dominant muscular dystrophy that results from small expansions of a polyalanine tract in the PABPN1 gene. Intranuclear inclusions are the pathological hallmark of OPMD. The mechanism by which protein aggregation in OPMD might relate to a toxic gain-of-function has so far remained elusive. Whether protein aggregates themselves are pathogenic or are the consequence of an unidentified underlying molecular mechanism is still unclear. Here, we report that protein aggregation in a cell model of OPMD directly impaires the function of the ubiquitin–proteasome pathway (UPP) as well as molecular chaperone functions. The proteasome inhibitor lactacystin causes significant increase of protein aggregation and toxicity. Moreover, overexpression of molecular chaperones (HSP40 and HSP70) suppressed protein aggregation and toxicity. We also provide evidence that mPABPN1–ala17 protein aggregation proportionally correlates with toxicity. Furthermore, we show that co-expression of chaperones in our OPMD cell model increases the solubility of mPABPN1-ala17 and transfected cell survival rate. Our studies suggest that molecular regulators of polyalanine protein solubility and degradation may provide insights into new mechanisms in OPMD pathogenesis. Further analysis of the cellular and molecular mechanisms by which UPP and molecular chaperones influence the degradation of misfolded proteins could provide novel concepts and targets for the treatment and understanding of the pathogenesis of OPMD and neurodegenerative diseases.

INTRODUCTION

Oculopharyngeal muscular dystrophy (OPMD) is an adult-onset autosomal dominant disease that affects skeletal muscles, especially those for eyelid elevation and swallowing. The OPMD locus was mapped by linkage analysis to chromosome 14q11.1 (1,2) and the gene was identified as PABPN1, which encodes for the poly (A) binding protein, nuclear 1 (PABPN1, PABII, PABP2) (3). The wild-type PABPN1 gene has a $(GCG)_6$ repeat encoding for alanine in the N-terminus of the protein, while OPMD patients show a short expansion of $(GCG)_{8–13}$ (3), which in turn leads to an expanded alanine tract. In PABPN1 $(GCG)_6$ codes for the first six alanines in a homopolymeric stretch of 10 alanines. OPMD is therefore associated with an expansion of a 12–17 uninterrupted alanine tract in the PABPN1 protein. In addition to OPMD, at least eight other diseases are associated with alanine stretch expansions in the disease gene products. (4–8).

The mechanism leading polyalanine-expanded PABPN1 to form aggregates associated with the disease is still unknown. One hypothesis is that the polyalanine stretches are able to adapt β-sheet structures, which leads to the formation of strong fibres extremely resistant to chemical denaturation and enzymatic degradation (9). Also, the expanded polyalanine tract in mPABPN1 may destabilize the native conformation of the protein, thereby causing it to misfold and aggregate. We previously observed that transient expression of the polyalanine expanded PABPN1 (mPABPN1–ala17) in COS-7 cells induces the formation of intranuclear inclusions (INIs) (10). It was reported that expression of 19 or 37 alanine repeats fused to GFP leads to INIs formation and increases cell death (11). In addition, our group showed that oligomerization of polyalanine expanded PABPN1

*To whom correspondence should be addressed at: Room L7-224, Montreal General Hospital, 1650 Cedar Avenue, Montreal, Quebec H3G 1A4, Canada. Tel: +1 5149348094; Fax: +1 5149348265; Email: guy.rouleau@mcgill.ca

facilitates INIs formation (12). We also demonstrated that preventing these INIs by inactivating oligomerization of mPABPN1–ala17 significantly reduces cell death. There is also the possibility that OPMD INIs sequester mRNA or other nuclear components and interfere with mRNA production, export and/or processing. The INIs found in the OPMD muscle fibers (13–15) were shown to sequester poly (A) RNA (13) and other nuclear proteins. Potential molecular mechanisms for OPMD pathogenesis were recently reviewed by our group (16).

The INIs formation in mPABPN1–ala17 may result from an imbalance between protein refolding and aggregation. Different observations converge to suggest that a gain of function of PABPN1 may cause the accumulation of nuclear filaments observed in OPMD (17). OPMD INIs are similar to those found in a number of inherited neurodegenerative diseases caused by mutated proteins with an expanded polyglutamine (polyQ) stretch. Many observations suggest that various types of inclusions arise through common mechanisms and elicit similar host responses. For example, all these inclusions contain components of the ubiquition–proteasome pathway (UPP) and also molecular chaperones, which represent the two main systems that protect cells against the buildup of unfolded polypeptides. The presence of these components in nuclear inclusions implies that the misfolded and aggregated protein is targeted for degradation (18–21). However, the presence of INIs suggests that mutant proteins are not adequately cleared by the UPP, and accumulate as a result.

Cells respond to toxic conditions by induction of a set of highly conserved genes that encode heat shock proteins (HSPs). Among the HSPs in eukaryotic cells are many molecular chaperones, which function to retard protein denaturation and aggregation, several antioxidant enzymes, which reduce oxidative damage to cell proteins, and components of the UPP (22–24). The UPP catalyzes the selective degradation of misfolded, unassembled or damaged proteins in the nucleus and cytosol that could otherwise form toxic aggregates (25–27). The relative importance of different protective mechanisms may depend on the nature of the mutated protein or the specific environmental stress.

Blocking the expression or accelerating the degradation of the toxic mPABPN1 protein may be an effective therapy of OPMD. It has been shown that reducing expression of the mutant polyglutamine containing protein in transgenic mice can reverse the phenotype (28). Other therapeutic strategies include inhibiting the tendency of the protein to aggregate (either with itself or with other proteins), up-regulating heat shock proteins that protect against toxic effects of misfolded protein, enhancing proteasome activity and blocking downstream effects, such as triggers of apoptosis.

Here we hypothesize that inclusion formation in OPMD is partly a consequence of insufficient proteasome and/or molecular chaperone function. We have found evidence that links the UPP and chaperone components in this disease; namely, we demonstrate that proteasome function is closely linked to aggregate formation, since treatment with the specific proteasome inhibitor lactacystin resulted in an enhancement of both nuclear and cytoplasmic protein aggregation. Furthermore, in the absence of lactacystin there seems to be no significant difference in expression levels of HSP70 between cells expressing wtPABPN1–ala10 and cells expressing mPABPN1–ala17, whereas upon treatment with the proteasome inhibitor we find a clear induction of HSP70 expression levels, as well as an increase in ubiquitin conjugates, exclusively in cells transfected with mPABPN1–ala17. Finally, we show that HSP40 and HSP70 may be involved in suppressing aggregation and toxicity in OPMD through modification of the solubility of the mutant protein. These results represent the first report of the direct involvement of the UPP pathway in modulation of aggregate formation and cell survival in OPMD.

RESULTS

Expression of mPABPN1–ala17 is sufficient to induce the formation of INIs

PABPN1 is an abundant nuclear protein that binds with high affinity to the poly (A) tail of mRNA, and is involved in mRNA polyadenylation (29). PABPN1 has 306 amino acids and comprises an alanine stretch and a proline-rich region in the N-terminus, an RNA binding domain in the central region, and a nuclear localization domain in the C-terminus (29).

We have established an *in vitro* model of OPMD using transfected Hela and COS-7 cells. In our model, mPABPN1–ala17 forms INIs in both cell lines (Fig. 1A and B).

Both HSP70 and ubiquitin are recruited into INIs of OPMD cell-based model and human tissue

Calado *et al.* (13) found that ubiquitin and the 20S proteasome co-localize to INIs in OPMD patient muscle (13). Recently, it was also demonstrated that components of the proteasome, HSP70, and ubiquitin co-localize to aggregates formed by mutated bovine PABPN1 in transfected COS-7 cells (30). To confirm the previous results, and to get a better comparison between HSP70 and ubiquitin redistribution into aggregates, we performed immunocytochemical staining on cells transfected with wtPABPN1–ala10 as well as mPABPN1–ala17. Figure 2A and C shows the uniform distribution of HSP70 and ubiquitin in cells transfected with wtPABPN1–ala10. A diffuse staining of both HSP70 and ubiquitin throughout the cytoplasm and nucleus was observed in these cells (Fig. 2A and C). Immunostaining was negative for the transfected green fluorescent protein (GFP) vector alone. In contrast, INIs of COS-7 and Hela cells transfected with mPABPN1–ala17 immunostained positively for both HSP70 and ubiquitin (Fig. 2B and D). These results confirm that HSP70 and ubiquitin have been redistributed to the INIs in our cell culture model. The presence of ubiquitin and HSP70 in the INIs supports the hypothesis that misfolded and aggregated proteins are targeted for proteolysis by the UPP. Together with the previous studies, our results provide evidence that polyalanine containing mPABPN1–ala17 elicits a stress response in cells.

To confirm the relevance of our findings in our cell model, we performed immunohistochemical staining on muscle sections of OPMD patients using the monoclonal HSP70 antibody. As shown in Figure 2E, INIs immunostained positively for the HSP70 in OPMD muscle cells. Muscles in control subject did not show immunostaining of subnuclear structures.

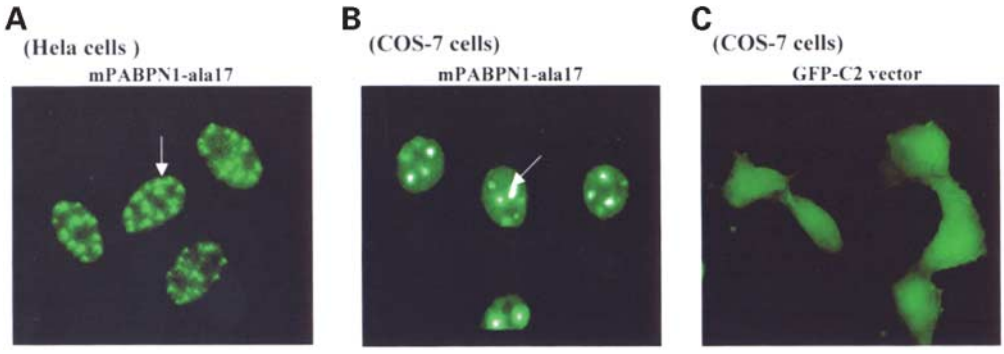

Figure 1. Expression of mPABPN1–ala17 in Hela and COS-7 cells induces insoluble intranuclear inclusions. Hela (**A**) and COS-7 (**B**) cells transiently transfected with mPABPN1–ala17. Forty-eight hours after transfection cells were fixed with 4% paraformaldehyde and then visualized using a fluorescence microscope. Arrows indicate the nuclei containing INIs induced by expression of mPABPN1–ala17. Cells transfected with control GFP-C2 vector alone are shown (**C**).

Proteasome inhibition by lactacystin increases mPABPN1–ala17 INI formation in a dose-dependent manner

The redistribution of ubiquitin and HSP70 into mPABPN1–ala17 positive INIs seems to suggest that INI formation may partly be a consequence of insufficient ubiquitin–proteasome and/or molecular chaperone function. To determine if this might be the case, we tested whether inhibition of the proteasome by lactacystin would promote polyalanine aggregation. We used the construct of mPABPN1–ala17, which leads to aggregation in our cell model, and we proceeded to quantify INI formation in the presence or absence of lactacystin. In untreated cells, mPABPN1–ala17 formed INIs in 40% of the total transfected cells. Treatment of transfected Hela or COS-7 cells with the specific proteasome inhibitor lactacystin, at a dose of 10 μM, led to a marked statistically significant increase in INIs formation (80%; $P < 0.05$). This increased INI formation occurred in a polyalanine size-dependent manner, since INI number did not vary in cells expressing wtPABPN1–ala10 (Fig. 5C). The increased number of INIs was associated with increased cell toxicity (data not shown). We also determined that INI formation was promoted by lactacystin in a dose-dependent manner, from 2.5 to 10 μM (Fig. 3A and B). Higher doses of lactacystin were lethal to cells. There was no difference in the transfection efficiency between cells incubated with or without lactacystin (Fig. 3A). We observed no difference in INI formation in control cells which were incubated with equivalent amounts of the carrier agent, dimethyl sulfoxide (DMSO), compared with cells transfected with mPABPN1–ala17 alone (Fig. 3B). We performed this experiment three independent times and calculated the number of cells containing INIs. The percentage of cells with INIs was obtained by dividing the number of cells with INIs by the total number of transfected cells. This was repeated three times for three different fields, then the average of the three ratios was computed and presented as a percentage (Fig. 3B).

Cytoplasmic inclusion formation is enhanced after lactacystin treatment of mPABPN1–ala17 transfected cells

Expression of mPABPN1–ala17 induces INI formation (Fig. 4A1 and A2). However, we were also able to detect a few cytoplasmic inclusions in cells transfected with mPABPN1–ala17 (Fig. 4A1). Moreover, inhibition of the proteasome by lactacystin at a dose of 10 μM seems to lead to an increase in cytoplasmic inclusion formation in COS-7 cells, as shown in Figure 4B, suggesting that these structures develop when a threshold of misfolded protein is exceeded. This is the first report showing the presence of cytoplasmic inclusions in cells transfected with mPABPN1–ala17. Based on our model, enhancing proteasome activity would thus be expected to reduce protein aggregation that is associated with cell death. A very recent report suggested that the proteasome activator REGg may be an attractive therapeutic target for neurodegerative diseases (31).

Lactacystin treatment increases the insoluble fraction of mPABPN1–ala17 protein

We previously demonstrated that the INIs induced by expression of mPABPN1–ala17 in COS-7 cells, as seen in OPMD patients, are insoluble and resistant to KCl treatment (12). To understand the mechanism by which protein aggregation is associated with increased cell death in OPMD (12), we sought to determine if lactacystin treatment alters the solubility of mPABPN1–ala17.

Protein extracts from cells transfected with mPABPN1–ala17 showed significant increase in insoluble fraction of mPABPN1–ala17 compared with cells transfected with wtPABPN1–ala10 (data not shown), when blotted with anti-PABPN1 antibody using a filter trap assay. The addition of lactacystin increased the insoluble fraction of mPABPN1–ala17 protein (Fig. 4D) and decreased the soluble fraction of mPABPN1–ala17 (data not shown): when cells transfected with mPABPN1–ala17 were incubated with 10 μM lactacystin for 24 h, the extracted proteins showed a distinct insolubility pattern, compared with the control cells transfected with mPABPN1–ala17 that were incubated with DMSO. This is consistent with previous studies reporting an increase in the aggregation of polyglutamine containing proteins in the presence of proteasome inhibitors (19,20).

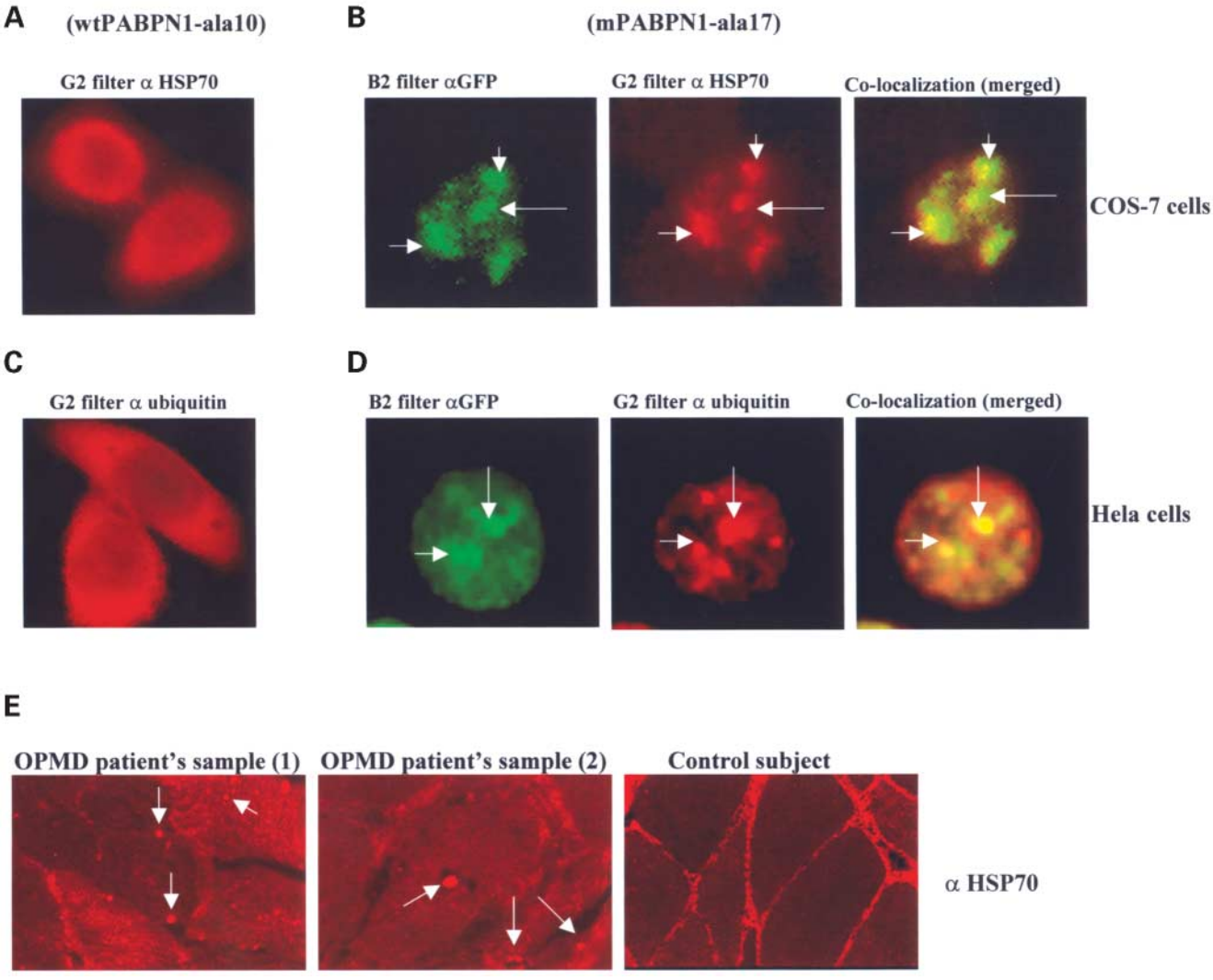

Figure 2. HSP70 and ubiquitin co-localize with INIs of mPABPN1–ala17 in cell culture model. HSP70 is recruited into INIs of OPMD muscle cells. Immunocytochemical detection on COS-7 and Hela cells transfected with GFP–wtPABPN1–ala10 and GFP–mPABPN1–ala17, 48 h post-transfection. CY3 conjugated secondary antibody (red) was used to label either HSP70 or ubiquitin. HSP70 and ubiquitin localize diffusely to the nucleus and cytoplasm in cells transfected with wtPABPN1–ala10 with no specific protein redistribution (**A** and **C**, respectively). In contrast, both HSP70 and ubiquitin co-localize to INIs of mPABPN1–ala17 (**B** and **D**, respectively). Merging (yellow) of the two signals (red and green) illustrates co-localization. Arrows indicate the INIs. (**E**) Immunohistochemical detection was performed on cross sections of the deltoid muscle from OPMD patients, using monoclonal anti-HSP70 antibody and CY3 conjugated secondary antibody. Nuclear inclusions stain positively for HSP70. Muscles in control subject did not show immunostaining of subcellular structures. Arrows indicate positively stained aggregates.

Lactacystin treatment leads to HSP70 and ubiquitin conjugate induction in cells transfected with mPABPN1–ala17

The inhibition of proteasomal function has been reported to induce the expression of HSP70 due to the accumulation of misfolded protein; therefore, we tested the possibility that the HSP70 is induced in our system. As shown in Figure 5A, lactacystin treatment increases both the constitutive HSP73 (upper band) and inducible HSP72 (lower band) forms of HSP70 in a dose dependent manner in cells transfected with mPABPN1–ala17. Equal amounts of proteins were loaded. A recent study reported that expression of HSP40 or HSP70 chaperones is induced under various conditions of cell stress, which results in unfolding and aggregation of certain proteins (32). To further confirm that lactacystin inhibition of proteasome activity leads to the increased aggregation that is associated with toxicity, anti-ubiquitin immunoblots were performed on cell lysates. Hela cells expressing mPABPN1–ala17 and incubated with lactacystin (at different doses) exhibited an increased level of total ubiquitinated conjugates. Bao *et al.* (30) demonstrated that incubation of cells which were transfected with PABPN1–ala17 with 0.4% DMSO for 24 h significantly reduced the proportion of cells with inclusions. In our study, we did observe that ubiquitin levels in cells transfected with mPABPN1–ala17 and treated with DMSO were lower than in cells transfected with mPABPN1–ala17 and treated with lactacystin. However, when we

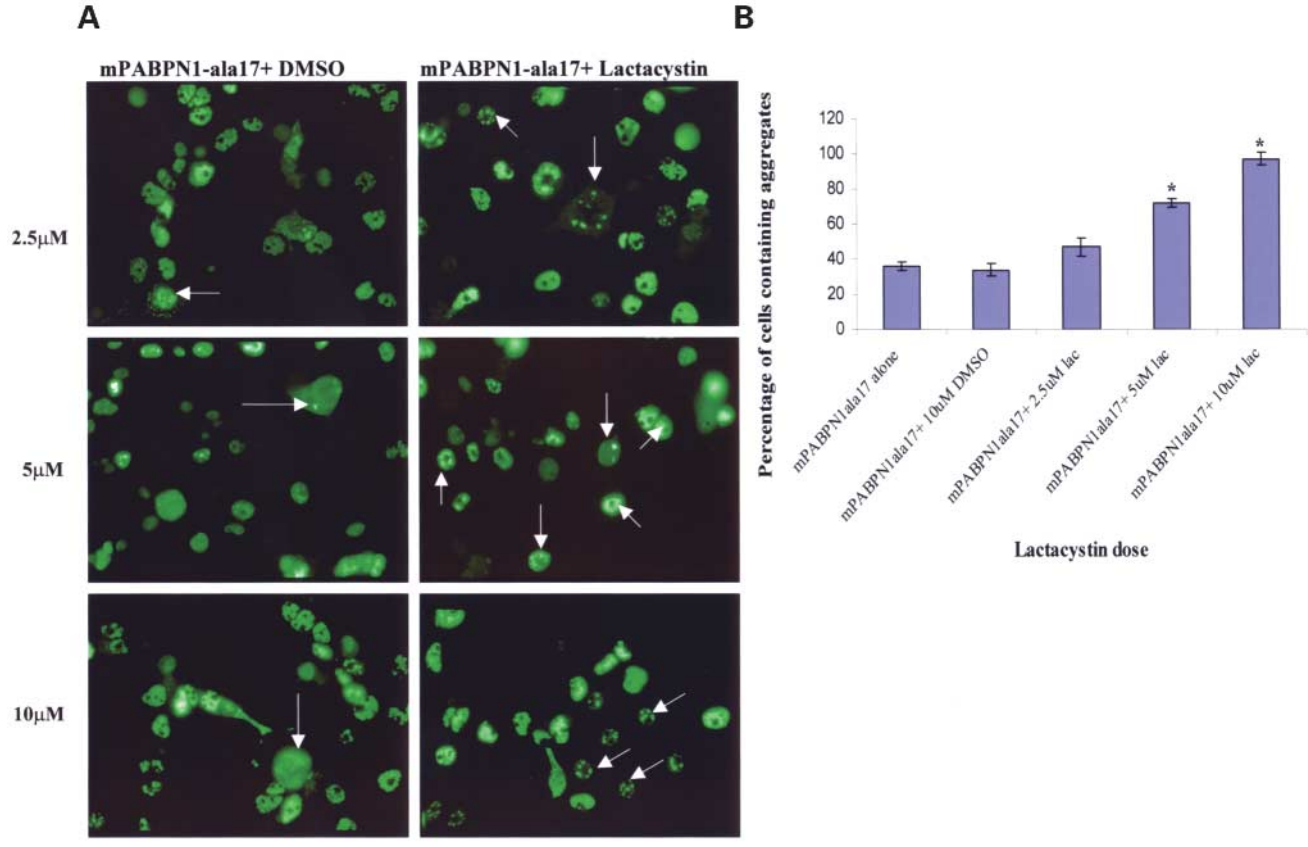

Figure 3. Lactacystin treatment increases INIs in cells transfected with mPABPN1–ala17 in a dose-dependent rate. (**A**) Immunofluorescence of COS-7 cells transfected with mPABPN1–ala17 and incubated with or without lactacystin (controls were treated with the carrier, DMSO). Lactacystin causes a marked increase in INIs. The arrows identify cells containing INIs or strong nuclear fluorescence signal. (**B**) Quantitation of lactacystin-induced mPABPN1–ala17 aggregation in COS-7 cells (2.5, 5 and 10 μM lactacystin) shows dose-dependence of lactacystin-induced aggregation. Cells were incubated for 24 h with the indicated concentrations of lactacystin and scored for INI formation. All transfected cells were scored by their staining pattern as having the nucleus diffusely labeled, or as containing nuclear aggregates. All experiments were repeated three times. All values were expressed as means ± SE. Statistical analysis was performed using the Anova single factor, with $*P < 0.05$ considered statistically significant.

examined the effect of DMSO alone, at different doses, on the total ubiquitin conjugates, we did not observe any increase in these bands compared with the cells expressing mPABPN1–ala17 alone or control non-transfected cells (Fig. 5B). Perhaps the difference in DMSO dose explains the discrepancies observed between the two studies. As shown in Figure 5B, there was a dramatic accumulation of ubiquitin immunoreactive bands only in cells transfected with mPABPN1–ala17 and treated with lactacystin. To address the issue that mPABPN1–ala17 is ubiquitinated and degraded by the proteasome, we examined whether there were alterations in the overall mPABPN1–ala17 protein level following treatment with lactacystin. As shown in Figure 5B, the level of mPABPN1–ala17 protein did not change with proteasomal inhibition. In the control non-transfected cells, there is a faint band corresponding to the endogenous PABPN1. To demonstrate equal protein loading, the blot was probed with anti-actin antibody.

Lactacystin has no effect on cells transfected with wtPABPN1–ala10

In our cellular model, wtPABPN1–ala10 can aggregate at high expression levels. However, the number and the size of the protein aggregates in mPABPN1–ala17 are significantly larger than in wtPABPN1–ala10. At lower expression levels, mPABPN1–ala17 formed significantly more aggregates compared to wtPABPN1–ala10 (Fig. 3A left panel, and Fig. 5C left panel); therefore we used low DNA concentrations in our transfection experiments for both wtPABPN1–ala10 and mPABPN1–ala17. Another group previously reported that both wtPABPN1–ala10 and mPABPN1–ala17 proteins can aggregate at high expression levels (30). However, it is worth mentioning that cells transfected with mPABPN1–ala17 in our model tend to die after 3 days, while cells transfected with wtPABPN1–ala10 die after 8 days (12, see also Fig. 6D). PABPN1 forms both linear filaments and discrete-sized, compact oligomeric particles *in vitro* (33) called speckles. We were able to detect speckles in cells transfected with both wtPABPN1–ala10 and mPABPN1–ala17. PABPN1 present in the intranuclear inclusions from OPMD patients is insoluble and resistant to KCl treatment, which is known to be able to dissolve soluble protein aggregates (13). Our group reported also that the aggregates induced by GFP–mPABPN1–ala17 are insoluble and remained after KCl treatment, whereas the GFP–wtPABPN1–ala10 signal is soluble and not resistant to KCl treatment (12).

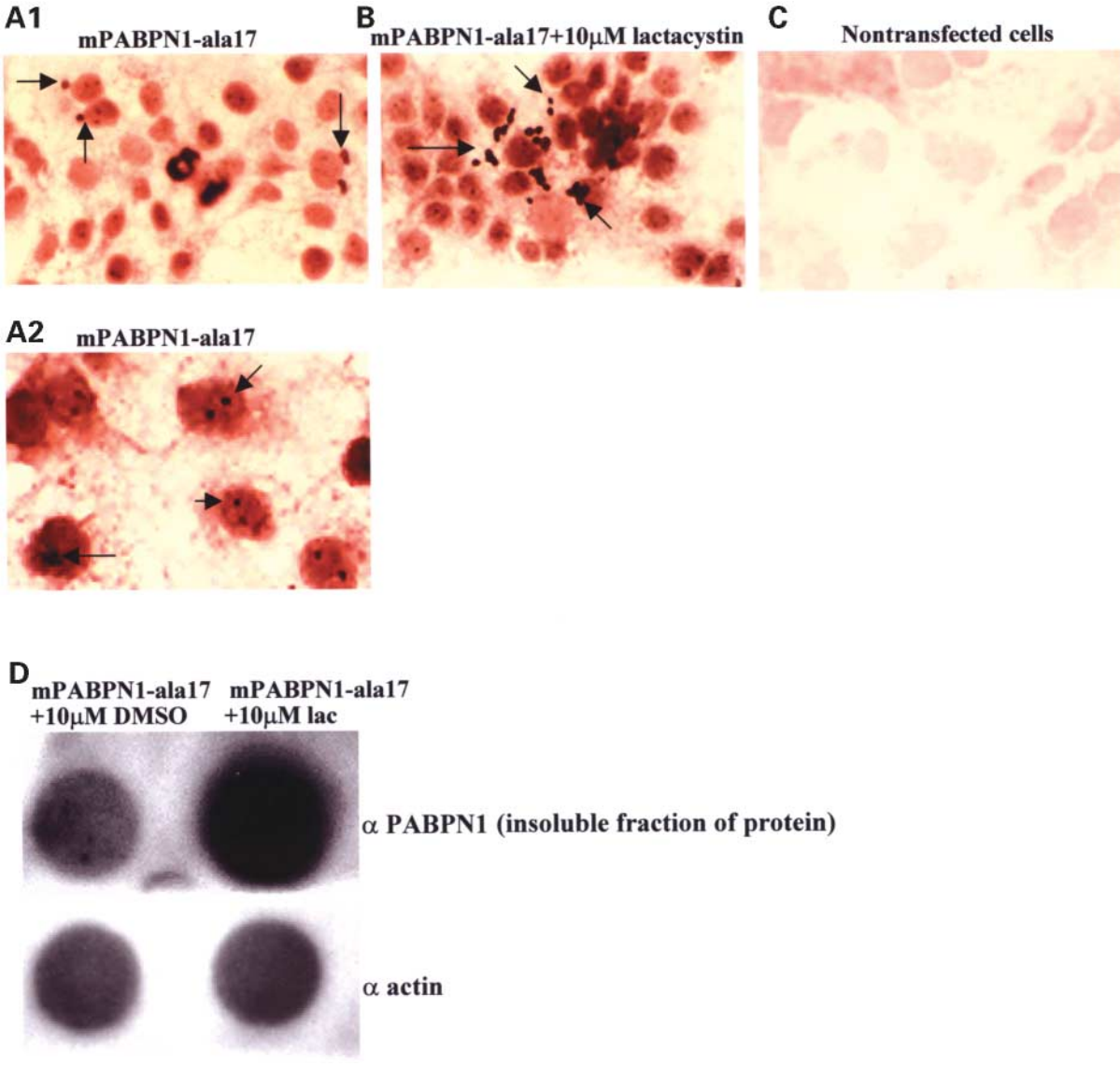

Figure 4. Lactacystin treatment enhances cytoplasmic inclusion formation in cells transfected with mPABPN1–ala17, and increases insoluble fraction of mPABPN1–ala17 protein. Immunocytochemistry of COS-7 cells transfected with mPABPN1–ala17 and incubated without or with lactacystin (**A** and **B**) and control cells (**C**). (**A1**) Expression of mPABPN1–ala17 induces INIs and some cytoplasmic inclusions. Arrows indicate cytoplasmic inclusions. (**A2**) Higher magnification of cell nuclei transfected with mPABPN1–ala17; arrows indicate nuclei containing INIs. (**B**) Lactacystin treatment of mPABPN1–ala17 promotes increased cytoplasmic inclusion formation, as well as nuclear inclusions. Arrows indicate nuclei flanked by cytoplasmic inclusions. (**C**) Control non-transfected cells. (**D**) Lactacystin treatment increases the insoluble fraction of mPABPN1–ala17 protein as shown by dot blot assay. Fractionation of lysates into insoluble fraction was carried before immunoblot analysis with anti-PABPN1 antibody. Equal loading of lysates was confirmed using anti-actin antibody.

Parallel sets of lactacystin treatment experiments were performed on cells transfected with wtPABPN1–ala10. No aggregation increase was observed after lactacystin treatment of cells transfected with wtPABPN1–ala10. Figure 5C shows the fluorescent micrographs of COS-7 cells transfected with wtPABPN1–ala10 and incubated with 10 μM lactacystin or 10 μM DMSO. There was no significant difference in aggregation formation in cells expressing wtPABPN1–ala10 following 10 μM lactacystin treatment compared with the control cells (Fig. 5C). Since aggregation was not increased in cells transfected with wtPABPN1–ala10, we conclude that the increased aggregate formation occurred only in cells transfected with mPABPN1–ala17. The effect of lactacystin treatment on cells transfected with wtPABPN1–ala10 was confirmed by measuring both HSP70 and ubiquitin levels. There was a slight change in HSP70 levels in cells expressing wtPABPN1–ala10 and treated with 10 μM lactacystin as compared to cells treated with DMSO (Fig. 5D). Equal amounts of protein were loaded.

It was also important to determine whether treating cells with lactacystin alone would induce HSP70. Therefore, we included the lysates from nontransfected cells, cells expressing wtPABPN1–ala10 and mPABPN1–ala17 in one blot and probed it with anti-HSP70 antibody. As shown in Figure 5D,

nontransfected cells treated with 10 μM lactacystin did not show any increase in HSP70 level. HSP70 induction was highly exclusively detected in cells expressing mPABPN1–ala17 and treated with 10 μM lactacystin (Fig. 5D). Anti-actin antibody was used to confirm that equal amounts of protein were loaded. Thus, we conclude that proteasome inhibition leads to ubiquitin conjugate and HSP70 induction only in cells transfected with mPABPN1–ala17.

HSP70 expression levels similar in both cells expressing wtPABPN1–ala10 and cells expressing mPABPN1–ala17

The recruitments of HSP70 to the INIs of OPMD prompted us to look for HSP70 chaperone induction by the expanded polyalanine mPABPN1–ala17. As shown in Figure 5D (lanes 3 and 5), in the absence of lactacystin there is no significant change of chaperone HSP70 induction level between cells expressing mPABPN1–ala17 and cells expressing wtPABPN1–ala10 (treated with control DMSO). One possible explanation is that the HSP70 chaperone is trapped in the insoluble inclusions of mPABPN1–ala17 preventing its activity. Another reason could be the aggregate burden: there is marked induction of HSP70 only when the aggregate burden is high, as it is in the cells transfected with mPABPN1–ala17 and treated with lactacystin (Fig. 5D).

Molecular chaperones (HSP40 and HSP70) suppress protein aggregation and cell toxicity of mPABPN1–ala17

Sittler *et al.* (34) demonstrated that huntingtin protein aggregation in cells can be suppressed by chemical compounds (geldanamycin) activating a specific heat shock response. Recently, several studies in fruit fly and mouse models in neurodegenerative disorders have provided direct evidence that molecular chaperones can suppress neurotoxicity (35–38). Based on polyglutamine disease literature (35–38), it seems plausible that HSPs might also have a role in OPMD pathogenesis.

To determine if molecular chaperones could modulate the frequency of aggregation in our cellular model, we co-expressed HSP40 and HSP70 with full-length mPABPN1–ala17, and determined the percentage of mPABPN1–ala17-expressing cells that contained INIs. As shown in Figure 6A, molecular chaperone HSP40 coexpression significantly decreased the aggregation frequency in our cell culture model. It was important to determine if the chaperones are altering total mPABPN1–ala17 protein expression levels, which may explain reduced INI formation. The level of mPABPN1–ala17 protein expression remained constant after co-expression with the chaperones: as shown in Figure 6B, HSP40 and HSP70 overexpression does not change the protein level of mPABPN1–ala17 when co-expressed in COS-7 cells. Anti-PABPN1 antibody was used as a primary antibody. Equal amounts of protein were loaded in each lane.

Quantification of protein aggregates was carried out (see Materials and Methods). HSP40 expression suppressed INI formation of mPABPN1–ala17 by ∼54%, while HSP70 expression showed a more modest effect of ∼30% reduction. The co-expression of both HSP40 and HSP70 with mPABPN1–ala17 seemed similar to the HSP40 alone (Fig. 6C). This may suggest that there is no significant synergistic effect of chaperones on aggregate suppression. Protein aggregation suppression, in our cell model, by chaperone overexpression is consistent with other studies of chaperone modulation of aggregation in polyglutamine expansion disorders (18,39,40), and seems to indicate functional effects of these chaperones in this cell culture system. The capacity of molecular chaperones to associate selectively with unfolded polypeptides facilitates substrate recognition by ubiquitin enzymes and perhaps degradation by the proteasome, reviewed by Sherman and Goldberg (41).

To determine whether chaperone overexpression could mitigate the toxicity of mPABPN1–ala17, we assessed the percentage of living cells every 24 h after transfection for a total of 7 days (Fig. 6D). The cells were counted every 24 h post-transfection. Each well was counted three times in different areas at one time point, and the mean was used for statistics. The percentage of living cells transfected represents the variation of the amount of living transfected cells at different time points compared with the number of transfected cells obtained on day 1 [mean ± SEM; $P < 0.05$ compared with any other groups (ANOVA analysis)]. Coexpression of HSP40 and HSP70 reduced mPABPN1–ala17 induced cell death at all time points tested. The cells transfected with mPABPN1–ala17 alone tend to die after 3 days. In the presence of either HSP40 or HSP70, the rate of cell survival was almost 40% higher ($P < 0.05$). The effect of both chaperones was similar to the HSP40 expression alone on cell survival (Fig. 6D). No significant synergistic effect of both chaperones was observed on mitigating toxicity. We therefore conclude that chaperone co-expression significantly reduces the cell toxicity of mPABPN1–ala17.

Modulation of mPABPN1–ala17 solubility by HSP40 and HSP70 chaperones

Increase in the expression levels of molecular chaperones offers new perspectives in the solubilization of proteins (42). The bulk of the available evidence supports an indirect role of chaperones in proteolysis, reflecting the ability of chaperones to maintain abnormal proteins in a soluble state (41–44). Since both HSP40 and HSP70 were significantly decreased INIs in our OPMD cell model, and cell survival increased was without altering the total mPABPN1–ala17 protein expression levels, we further analyzed the effects of these chaperones on the biochemical properties of mPABPN1–ala17. To understand the mechanism by which the chaperones suppress aggregation, we sought to determine if these chaperones alter the solubility of mPABPN1–ala17 protein. First, we analyzed the solubility of both wtPABPN1–ala10 and mPABPN1–ala17 using a filter trap assay. As shown in Figure 7A, the expression of wtPABPN1–ala10 shows a significant higher level of soluble protein compared with mPABPN1–ala17 expression. The dot blot was probed with anti-PABPN1 antibody. Probing with an anti-actin antibody confirmed that equivalent amounts of protein were loaded. Second, we studied the effect of chaperone coexpression on modulation of mPABPN1–ala17 solubility. Soluble and insoluble mPABPN1–ala17 levels in cells where chaperones are coexpressed (filter trap assay) are shown in Figure 7B. The expression of HSP40 or HSP70 resulted in a

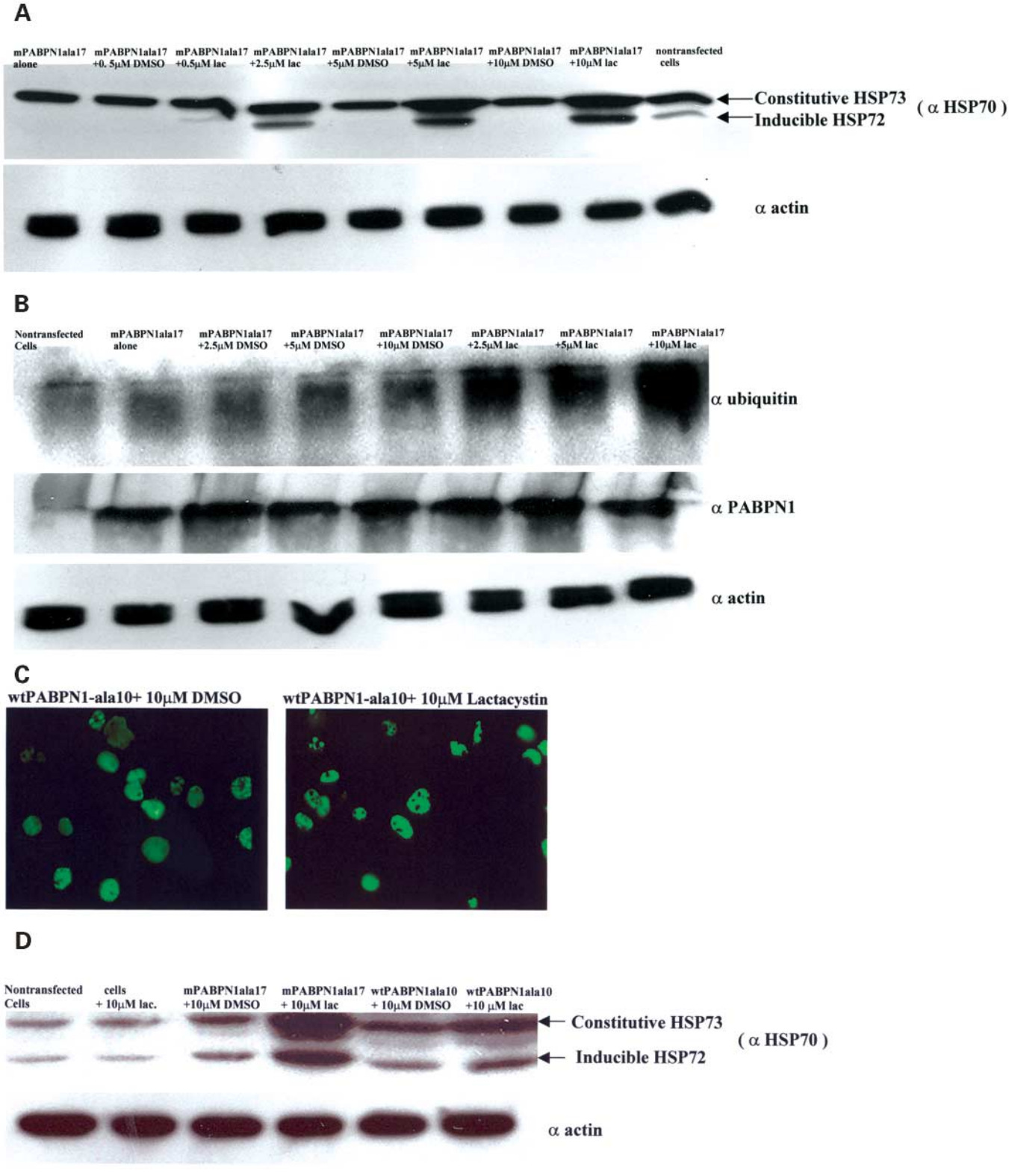

significant increase in soluble mPABPN1–ala17 compared with mPABPN1–ala17 coexpressed with control vector. To further confirm these results, we also showed a significant decrease in insoluble mPABPN1–ala17 when coexpressed with the chaperones, compared with mPABPN1–ala17 coexpressed with control vector (Fig. 7B). Equal amounts of the lysates were loaded. This may suggest proteasome degradation involvement after chaperone overexpression. It was necessary to confirm that chaperone overexpression did not change the mPABPN1–ala17 levels in the transfected Hela cells, using the filter trap assay. As shown in Figure 7C, the level of mPABPN1–ala17 remained constant after HSP40 and/or HSP70 overexpression. The same results were obtained using different co-transfection ratios (mPABPN1–ala17 : chaperone; 1 : 4 and 1 : 3) using anti-PABPN1 antibody. The dot blot assay in Figure 7C confirms the previous results shown in Figure 6B. We therefore conclude that the effect of chaperones on reducing mPABPN1–ala17 INIs and toxicity acts through modulation of mPABPN1–ala17 solubility, and conformation stabilization, and not by reducing mPABPN1–ala17 expression level.

DISCUSSION

We have presented evidence that the UPP and molecular chaperones are part of the cellular response to mutant polyalanine-containing PABPN1.

The recruitment of UPP and chaperone molecules into INIs may represent an effort by the cell to clear the misfolded mPABPN1–ala17. Intracellular aggregation of polyglutamine proteins has been suggested to impair the UP system (45,46). Once the β-sheet oligomers of mPABPN1–ala17 are initiated, ubiquitin, molecular chaperones and proteasome regulatory complexes may become unable to refold or degrade these oligomers, and hence trapped in the INIs. This trapping of UP particles may result in a partial inhibition of proteasomal activity and eventually cellular dysfunction. Both HSP40 and HSP70 have been reported to be localized predominantly in the cytoplasm before heat shock and relocalize to the nucleus after heat shock (47,48). The presence of HSP70 in mPABPN1–ala17 INIs may reflect a stress response. However, a recent study showed that polyglutamine protein aggregates are dynamic structures and that molecular chaperones are not sequestered into aggregates, but are instead transiently associated (49).

The proteasome inhibition data presented here are the first evidence showing a direct link between the role of proteasome function and OPMD. Our findings that proteasome inhibition increases protein inclusion formation imply that proteasome activity may play an important role in modulating aggregation in OPMD. Ravikumar *et al.* (50) also demonstrated that epoxomicin (another proteasome inhibitor) increased the proportion of COS-7 cells expressing GFP–ala19 aggregates. They also noted a marked increase in HSP70 on epoxomicin treatment, consistent with inhibition of the proteasome. These and our results are consistent with those obtained for polyglutamine diseases, where treatment of transfected cells with proteasome inhibitors resulted in greater accumulation of polyglutamine polypeptides, increase in the number of inclusion bodies and enhanced apoptosis (18–20). We examined whether there were alterations in the levels of mPABPN1–ala17, following proteasome inhibition, as would be expected if it is normally degraded through the proteasome. We did not detect any changes in mPABPN1–ala17 protein levels. It is possible that aggregated mPABPN1–ala17 is not soluble even in SDS buffer. Alternatively, mPABPN1 may not be degraded exclusively by the proteasome. We cannot exclude the possibility that mPABPN1–ala17 could also be targeted to the lysosomal pathway. A recent study showed that antifungal antibiotic (rapamycin) enhanced the clearance of GFP–ala19-associated aggregates (50), suggesting the autophagy–lysosomal pathway as an alternative degradation system.

Lactacystin promoted aggregation of full-length mPABPN1–ala17. In the presence of lactacystin, mPABPN1–ala17 formed more cytoplasmic, perinuclear aggregates as well as INIs, whereas under control conditions it formed exclusively INIs. The formation of cytoplasmic inclusions, despite the presence of nuclear localization signal (NLS) in mPABPN1–ala17 (Fig. 4B), suggests that lactacystin caused mPABPN1–ala17 to aggregate before it could be transported to the nucleus, essentially trapping the protein in the cytoplasm.

We have recently shown that oligomerization of mPABPN1–ala17 facilitates nuclear protein aggregation of OPMD (12). When proteasome activity is blocked with lactacystin or other inhibitors, the concentration of misfolded polyalanine protein would increase, favoring oligomerization and aggregation. In

Figure 5. Proteasome inhibitor (lactacystin) treatment leads to ubiquitin conjugate and HSP70 induction only in cells transfected with mPABPN1–ala17. (**A**) lysates from control cells and cells expressing mPABPN1–ala17 in the absence or presence of lactacystin (0.5, 2.5, 5 and 10 μM) were examined; immunoblotting with anti-HSP70 antibody showed increase in both the constitutive HSP73 (upper band) and inducible HSP72 (lower band) forms of HSP70 after lactacystin treatment. Equal loading of proteins was confirmed using anti-actin antibody. (**B**) Hela cells expressing mPABPN1–ala17 and incubated with different doses of lactacystin (2.5, 5 and 10 μM) exhibited an increased level of total ubiquitinated conjugates, compared with the controls, as shown by western blot using anti-ubiquitin antibody. Control cells were transfected with mPABPN1–ala17 and treated with the carrier, DMSO, at similar doses of lactacystin. Cells expressing mPABPN1–ala17 alone as well as non-transfected cells are also shown. Total ubiquitin conjugate levels remained constant in cells expressing mPABPN1–ala17 and treated with DMSO at different doses. Similar ubiquitin conjugate levels were observed in cells expressing mPABPN1–ala17 alone or non-transfected cells. The blot was re-probed with anti-PABPN1 antibody to measure PABPN1 protein levels: PABPN1 expression level did not change after lactacystin treatment in cells expressing mPABPN1–ala17. Note the faint band of the non-transfected cells that corresponds to the endogenous PABPN1 protein. Equal loading of proteins was confirmed using anti-actin antibody. There was no clear HSP70 induction in cells expressing mPABPN1–ala17 compared with cells expressing wtPABPN1–ala10. (**C**) Green fluorescent micrographs of COS-7 cells transfected with wtPABPN1–ala10 and incubated with 10 μM DMSO or 10 μM lactacystin. There was no difference in aggregation formation in cells expressing wtPABPN1–ala10 following lactacystin treatment compared to the control cells. (**D**) Lysates from nontransfected cells, cells expressing wtPABPN1–ala10 and mPABPN1–ala17 were examined by immunoblot with anti-HSP70 antibody. The lysates from cells were treated with 10 μM DMSO or 10 μM lactacystin. Lactacystin did not induce HSP70 in non-transfected cells. HSP70 induction was highly detected in cells expressing mPABPN1–ala17 and treated with 10 μM lactacystin. There was a slight change in HSP70 level in cells expressing wtPABPN1–ala10 and treated with 10 μM lactacystin. Equal loading of proteins was confirmed using anti-actin antibody.

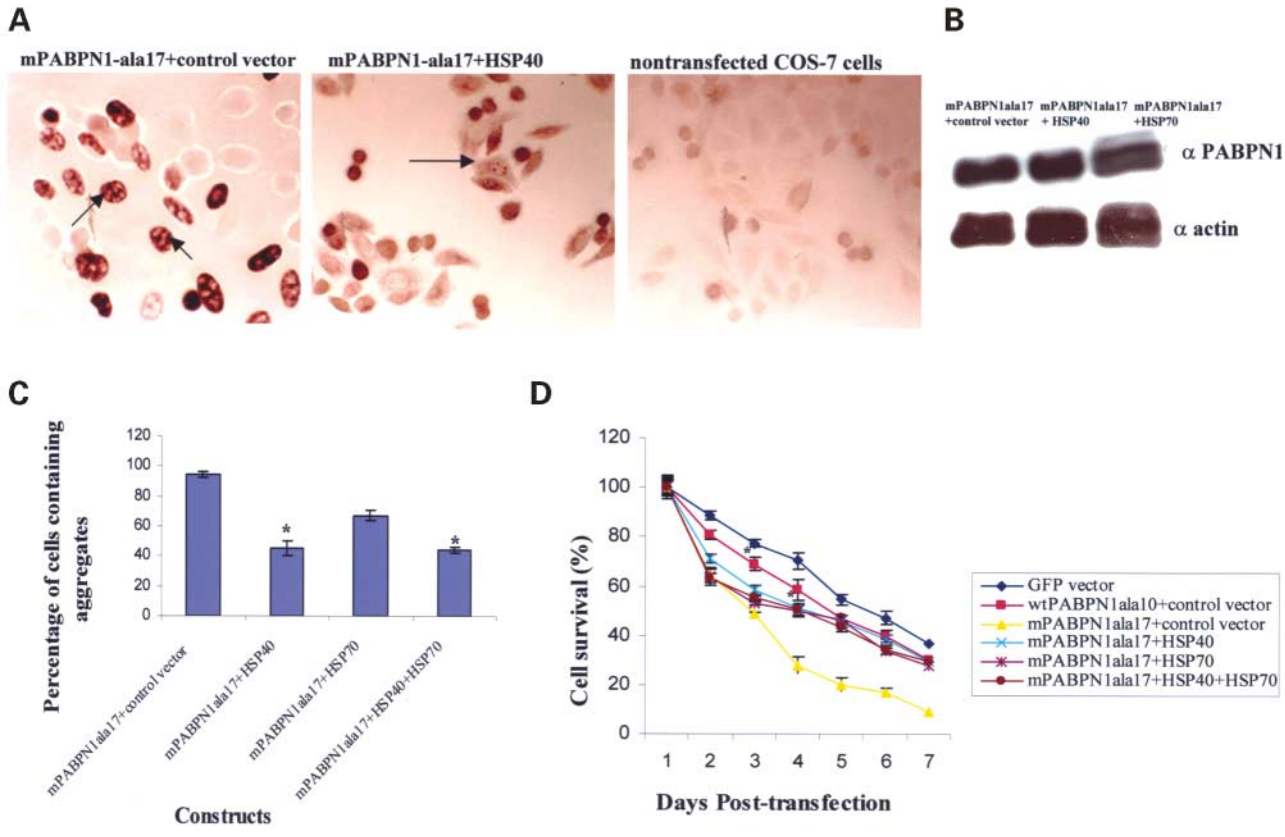

Figure 6. Molecular chaperone overexpression reduces INIs and cell toxicity of mPABPN1–ala17 without affecting protein expression levels. (**A**) Immunocytochemistry of COS-7 cells co-transfected with mPABPN1–ala17 and control vector shows cells containing INIs. We found significant reduction of INIs in cells co-transfected with mPABPN1–ala17 and HSP40. Non-transfected cells were used as control. Arrows indicate the transfected cells containing insoluble INIs. (**B**) Molecular chaperone HSP40 overexpression does not change the protein level of mPABPN1–ala17 when co-transfection in COS-7 cells was carried out as shown by western blot. Anti-PABPN1 antibody was used as primary antibody. Equal amounts of protein were loaded in each lane. Experiment was repeated three times, all showing that the chaperones (HSP40 or HSP70) do not alter total mPABPN1–ala17 protein level. (**C**) COS-7 cells co-transfected with mPABPN1–ala17 along with control vector or HSP40, HSP70, HSP40 and HSP70 expressing vectors. The proportions of GFP-positive cells with INIs were determined at 48 h post-transfection. The results come from three representative independent experiments. Mean ± SEM; $*P < 0.05$ (ANOVA analysis). (**D**) Percentage of living cells expressing co-transfected constructs at different times post-transfection. COS-7 cells co-transfected with wtPABPN1–ala10 or mPABPN1–ala17 and control vector or HSP40, HSP70, HSP40 and HSP70 expression vectors. The cells were counted every 24 h post-transfection. Each well was counted three times in different areas at one time point, and the mean was used for statistics. The percentage of living cells transfected represents the variation of the amount of living transfected cells at different time points compared with the number of transfected cells obtained on day 1. Mean ± SEM; $*P < 0.05$ compared with any other groups (ANOVA analysis).

order to be degraded by the proteasome, a protein must first be unfolded to be able enter the central proteolytic chamber. mPABPN1–ala17 may form a highly insoluble stable β-sheet that resists unfolding and thus blocks entrance to the chamber. Alternatively, proteasome inhibitors could increase polyalanine aggregation indirectly through effects on other cellular processes, such as induction of the apoptosis pathway. The higher the concentration of hydrophobic amino acid chains in the protein, the more likely it is that protein aggregation occurs (42). The fate of the misfolded mPABPN1–ala17 would reflect the relative affinities of non-native protein for proteases or chaperones and the relative rates of degradation, aggregation and folding.

The cellular defenses against unfolded proteins, including UPP and molecular chaperones, are highly inter-linked. We found that lactacystin treatment led to an increase in ubiquitin and HSP70 levels in cells transfected with mPABPN1–ala17. Our results suggest that polyalanine aggregation may be necessary, but not sufficient, to elicit a stress response. There is marked HSP induction only when the aggregate burden is high, as it is after lactacystin treatment. Various observations indicate that aged organisms and senescent cultures of mammalian cells are less able to induce HSPs in response to protein-damaging conditions (51,52). The late onset of OPMD implies that the affected muscles can deal successfully with the mutant PABPN1 for many years. We suggest that one possible factor contributing to the development of symptomatic OPMD is a reduced capacity of cells from older individuals to cope with abnormal expanded PABPN1. As a consequence of decreased HSP inducibility, the expanded polyalanine-containing PABPN1 builds up in cells of aged individuals to higher levels and results in greater tendency to form insoluble INIs, and may lead to cell death.

According to the literature, most chaperones bind to peptide segments that are enriched in hydrophobic amino acids (42), which are found in the core of native proteins. One possible explanation for the impairment of chaperone function in OPMD is that in mPABPN1–ala17 the expanded polyalanine

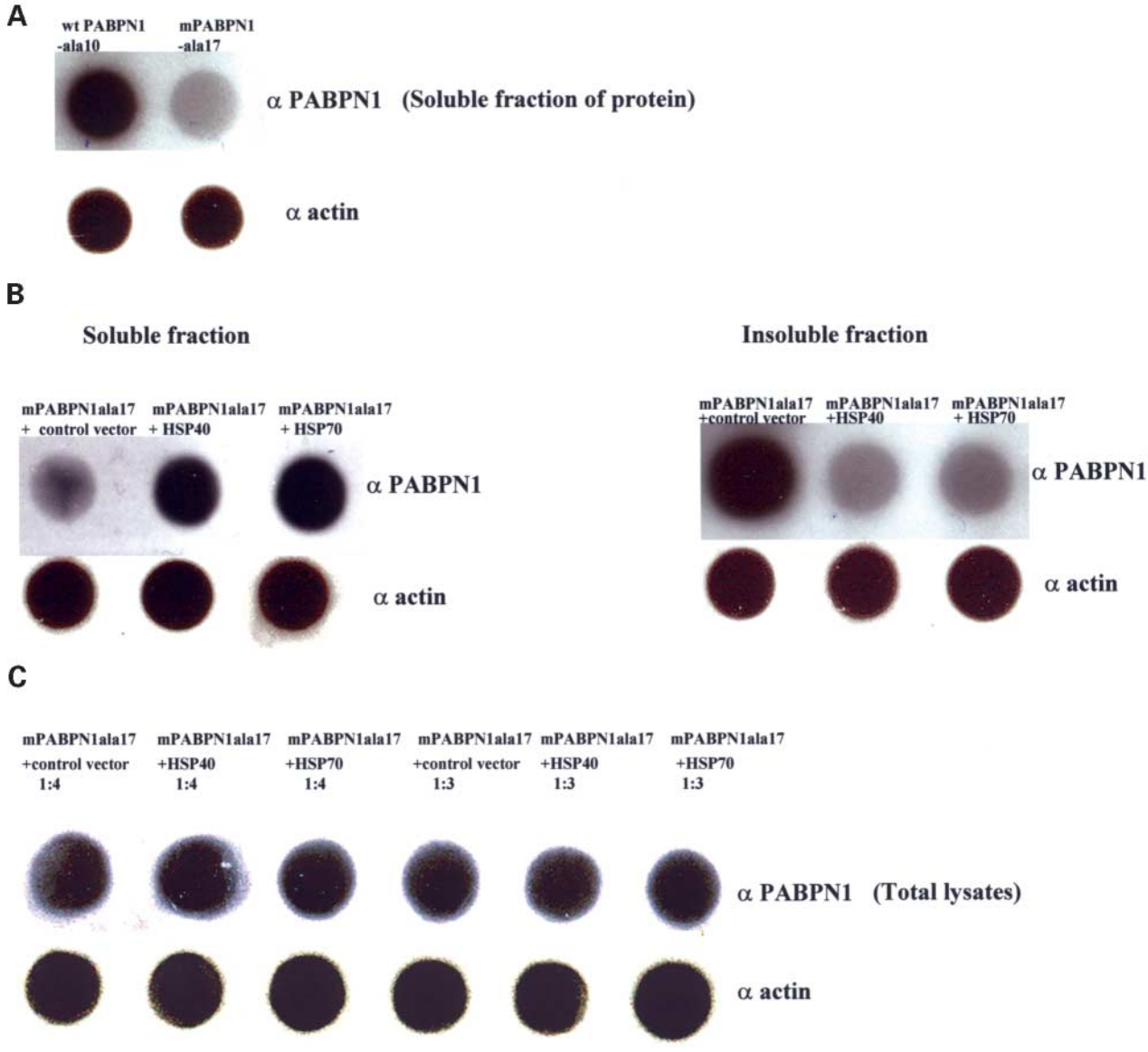

Figure 7. Molecular chaperone overexpression increases soluble fraction of mPABPN1–ala17 protein without affecting the level of mPABPN1–ala17 protein. (**A**) The expression of wtPABPN1–ala10 shows a significant more soluble protein level when compared with mPABPN1–ala17 expression. Nitrocellulose dot-blot was used to detect soluble fraction of the protein. Immunoblotting was performed using anti-PABPN1 antibody. Probing with an anti-actin antibody confirmed that equivalent amounts of the protein were loaded. (**B**) Detection of soluble and insoluble fractions of mPABPN1–ala17 after chaperone co-transfection. Overexpression of HSP40, or HSP70 with mPABPN1–ala17 increases the soluble fraction of mPABPN1–ala17 protein as shown in dot blot assay. The increase in soluble protein was accompanied by a concomitant decrease in the insoluble mPABPN1–ala17 protein. Transfected Hela cells were harvested and fractionation of lysates into soluble and insoluble fractions was carried out before immunoblot analysis with anti-PABPN1 antibody. Equal loading of lysates was confirmed using anti-actin antibody. (**C**) Molecular chaperone overexpression does not change the protein level of mPABPN1–ala17 when co-transfection of Hela cells was carried out at different ratios (mPABPN1–ala17:chaperone, 1 : 4 or 1 : 3). The filter membrane was blotted with anti-PABPN1 antibody. Equal loading of lysates was confirmed using anti-actin antibody. The filter trap assay experiments were performed three times.

tracts form β-sheet structures whose stability exceeds the capacity of chaperones to disaggregate and refold the protein to the active conformation. Molecular chaperone overexpression may prevent protein aggregation directly by shielding the interactive surfaces of nonnative polyalanine and indirectly by inhibiting intramolecular β-sheet conformation and thus block ordered oligomerization. Another possibility is that overexpression of chaperones enhances the function of the UPP for mPABPN1–ala17 degradation because the function of the UPP is related to the expression level of chaperones (53).

The finding that molecular chaperones suppress the aggregation and toxicity associated with polyglutamine disease models and enhance the protein solubility (18,20,21,37,38,42–44,54–56) formed the basis for our studies aimed at better understanding their effects. First, we have confirmed previous data (30) showing that both HSP40 and HSP70 suppress

protein aggregation and toxicity associated with mutated bovine PABPN1–ala17. Second, we examined the effect of chaperones on the solubility of mPABPN1–ala17. Our data reveal that the overexpression of either HSP40 or HSP70 enhances the solubility of mPABPN1–ala17, while not affecting mPABPN1–ala17 expression levels. Therefore, suppression of OPMD protein aggregation by molecular chaperones may occur through alteration of mPABPN1–ala17 solubility and conformational correction, rather than reducing levels of mPABPN1–ala17. Furthermore, our results suggest that enhanced solubility of mPABPN1–ala17 by molecular chaperones may increase the cell survival in OPMD. The increase in soluble mPABPN1–ala17 protein was accompanied by a concomitant decrease in the insoluble mPABPN1–ala17 protein when coexpressed with the chaperone. These observations suggested that overexpression of HSP40 or HSP70 enhanced the function of the UPP and subsequently accelerated the degradation of mPABPN1–ala17 protein. The UPP, particularly its activity, is related to chaperone expression levels (53). A very recent paper demonstrated that HSP70 overexpression ameliorates spinal and bulbar muscular atrophy phenotypes in mice by reducing nuclear-localized mutant androgen receptor, probably caused by enhanced mutant androgen receptor degradation (56). Another recent report showed that increased levels of HSP70 and HSP90 promote tau solubility and tau binding to microtubules in tau transgenic mouse and Alzheimer's disease brains, suggesting that HSP70 may help to recruit misfolded proteins as substrates for parkin E3 ubiquitin ligase activity (57). A recent finding indicated that HSP70 enhances parkin binding and ubiquitination of expanded polyglutamine protein *in vitro* (58). Based on the chaperone solubility results, we tested the effect of lactacystin, a proteasome inhibitor, on mPABPN1–ala17 solubility. We found that significant increase in protein aggregation after lactacystin treatment is accompanied by an increased level of the insoluble form of mPABPN1–ala17. These results demonstrate that insolubility of mPABPN1–ala17 renders the protein more toxic to the cells. Our observations may be the basis for a possible strategy for OPMD treatment. Also, the finding that protein aggregation is not a dead-end in the life cycle of a protein could be used in the design of therapies for this and similar diseases: use of the bichaperone system may avoid the treatment of inclusion bodies with strong denaturing agents and may promote folding into the biologically active protein conformation.

MATERIALS AND METHODS

Plasmid construction

The cDNAs encoding wtPABPN1 with 10 alanines (wtPABPN1–ala10) and mPABPN1 with 17 alanines (mPABPN1–ala17, as seen in OPMD patients) were cloned into the pEGFP-C2 vector (Clontech, Palo Alto, CA, USA), resulting in a fusion of GFP to the N-termini of PABPN1 proteins. pFlag-CMV-2-HSP40 and pcDNA3.1/HisA-HSP70 expression vectors were kindly provided by Dr Huda Zoghbi (Baylor College of Medicine, Houston, TX, USA) (17). All constructs were validated by DNA sequencing.

Cell culture and transfection

Twenty-four hours before transfection, COS-7 or Hela cells were seeded in Dulbeco's modified Eagle's medium (DMEM) (Gibco BRL, MD, USA) containing 10% fetal calf serum (Gibco BRL) at a concentration of 2×10^5 cells per well in six-well plates containing sterile cover slips. The cells were transfected with plasmid DNA (2.0 μg) using Lipofectamine reagent (Gibco BRL) according to the manufacturer's instructions. For co-transfection experiments, pFlag–CMV-2 expressing full-length human HSP40 and/or pcDNA3.1/HisA expressing full-length human HSP70 were co-transfected with GFP–wtPABPN1–ala10 or GPF–mPABPN1–ala17 constructs at 4:1 ratio. Cells were transfected with 0.4 μg of GFP construct and 1.6 μg of the appropriate chaperone or control (empty) vector DNA per well, to ensure that all cells expressing the GFP fusion proteins also expressed the appropriate chaperone proteins. Different ratios of co-transfection (chaperone: mPABPN1–ala17; 3 : 1, 2 : 1) were examined and fixation was performed 48 h post-transfection with 4% paraformaldehyde; cells were then visualized using a fluorescence microscope with a filter appropriate for GFP in three independent experiments.

Proteasome inhibitor treatment

Twenty-four hours after transfection, cells were incubated with the proteasome inhibitor lactacystin (lac.; Calbiochem, La Jolla, CA, USA) for a further 24 h. The results shown in Figure 3B are from three representative independent experiments. The concentration used was 10 μM lactacystin (unless otherwise stated). Control cells were incubated with equivalent amounts of the carrier agent, DMSO.

Immunocytochemistry and immunohistochemistry

Fourty-eight hours after transfection, cells were washed with PBS, fixed for 15 min. with 4% paraformaldehyde, permeabilized for 5 min with 0.05%Triton-X/PBS, then blocked with 10% normal goat serum (NGS)/PBS. Cells were incubated overnight in primary antibody in the following dilutions: α GFP = 1 : 500; α PABPN1 = 1 : 100; α ubiquitin = 1 : 1000; α HSP70 = 1 : 1000. For colorimetric detection, cells were washed three times in PBS, and then incubated for 1 h in appropriate biotinylated secondary antibody (1 : 500). After three PBS washes, amplification was carried out using the ABC Elite kit (Vector). Cells were incubated for 1 h, and the reaction product was visualized using the VIP (Vector) kit. Coverslips were then mounted on slides. For fluorescent detection experiments, cells were incubated in the appropriate secondary fluorescent antibody (CY3, 1 : 300), washed, and then mounted in Slow-Fade Mount (Molecular Probes, Eugene, OR, USA). Cells were visualized using appropriate filters on a Leica Polyvar microscope.

The microtome sections of paraffin-embedded deltoid muscle from OPMD patients and a control subject were used (kindly provided by Dr G. Karpati, MNI). Sections were deparaffinized, permeabilized and immunostained with monoclonal antibody against HSP70. Rhodamine conjugated secondary antibody was used and the signal was visualized using a

fluorescent microscope. The concentration of anti-HSP70 antibody (Chemicon) was 1 : 300.

Western blotting

Fourty-eight hours after transfection cells were harvested and protein was extracted in lysis buffer. Equal amounts of protein were electrophoresed on 12% SDS–PAGE and transferred to a nitrocellulose membrane. The membranes were probed with a monoclonal anti-GFP antibody (Clontech, 1 : 1000), polyclonal anti-PABPN1 antibody (1 : 100), anti-HSP70 antibody (1 : 1000) and anti-ubiquitin antibody (1 : 100) and detected using the western blot chemiluminescence reagent *Plus* kit (NEN Life Science Products, Boston, MA, USA). Parallel samples were probed with anti-actin antibody to verify equal loading of lysates.

Quantitation of aggregates and cell viability

Quantitation of aggregates in transfected cells was carried out by an observer blind to the treatment conditions. All transfected cells were scored by their staining pattern as having the nucleus diffusely labeled, or as containing nuclear aggregates. The percentage of cells with INIs was obtained by dividing the number of cells with INIs by the total number of transfected cells. This was repeated three times for three different fields, and then the average of the three ratios was computed and presented as a percentage.

For cell toxicity assay, the number of living cells was measured every 24 h post-transfection, for a total of 7 days. Briefly, each well was washed with DMEM to remove detached cells and the cells expressing GFP were counted in a 1 mm^2 area under low magnification (25×). Three different areas were counted for each well. All wells were in duplicate and the experiments were repeated three times ($n = 6$). All values were expressed as means ± SE. Statistical analysis was performed using the Anova single factor, with $P < 0.05$ considered statistically significant.

Solubility analysis by filter retardation assay

Since insoluble mPABPN1–ala17 cannot be adequately quantified by western blotting (12), we used a filter trap assay (59,60) for quantitative analysis of insoluble form of the mutant PABPN1.

For solubility studies, transfected cells were harvested and resuspended for 20 min on ice in non-denaturing SDS lysis buffer (10 mM Tris pH 8.0, 150 mM NaCl, 2% SDS, supplemented with protease inhibitors PMSF and pepstatin). Samples were fractionated by centrifugation at 16 000*g* for 10 min. The supernatant (soluble fraction) was then transferred to a separate tube. The insoluble pellet was resuspended in an equal volume of lysis buffer for 10 min, and sonicated briefly. The supernatant and the pellet fractions represent the soluble and insoluble fractions of the extract, respectively. Equal amounts of supernatant and pellet fractions were then analyzed by filter trap assay. The filter trap assay (59,60) was performed with 0.45 µM nitrocellulose (Schleicher and Schuell, Dassel, Germany), and two pieces of Whatman filter paper to support the membrane, using a dot-blot apparatus. The membrane was washed twice with washing buffer (0.1% SDS, 10 mM Tris, pH 8.0, 150 mM NaCl). Samples were prepared in a final volume of 100 µl in lysis buffer, boiled for 3 min, and equal amounts of protein extracts were loaded. The membrane was washed twice with wash buffer, and then removed from the apparatus. Dot-blots were probed as described above for western blots.

ACKNOWLEDGEMENTS

We thank Simon Laganiere for valuable help in figure and manuscript preparation.We thank Dr Huda Zoghbi for providing the human HSP40 and HSP70 constructs. We also thank Dr George Karpati for providing us with the OPMD patient samples. We are grateful to Dr Patrick Dion for his technical help with the filter trap assay. This work was supported by the Muscular Dystrophy Association (MDA), the Canadian Institute of Health Research and the Federation Foundation of Greater Philadelphia.

REFERENCES

1. Brais, B., Xie, Y.G., Sanson, M., Morgan, K., Weissenbach, J., Korczyn, A.D., Blumen, S.C., Fardeau, M., Tome, F.M., Bouchard, J.P. and Rouleau, G.A. (1995) The oculopharyngeal muscular dystrophy locus maps to the region of the cardiac alpha and beta myosin heavy chain genes on chromosome 14q11.2–q13. *Hum. Mol. Genet.*, **4**, 429–434.
2. Xie, Y.G., Rochefort, D., Brais, B., Howard, H., Han, F.Y., Gou, L.P., Maciel, P., The, B.T. Larsson, C. and Rouleau, G.A. (1998) Restriction map of a YAC and cosmid contig encompassing the oculopharyngeal muscular dystrophy candidate region on chromosome 14q11.2–q13. *Genomics*, **52**, 201–204.
3. Brais, B., Bouchard, J.P., Xie, Y.G., Rochefort, D.L., Chretien, N., Tome, F.M., Lafreniere, R.G., Rommens, J.M., Uyama, E., Nohira, O. *et al.* (1998) Short GCG expansions in the PABP2 gene cause oculopharyngeal muscular dystrophy. *Nat. Genet.*, **18**, 164–167.
4. Muragaki, Y., Mundlos, S., Upton, J. and Olsen, B.R. (1996) Altered growth and branching patterns in synpolydactyly caused by mutations in HOXD13. *Science*, **272**, 548–551.
5. Mundlos, S., Otto, F., Mundlos, C., Mulliken, J.B., Aylsworth, A.S., Albright, S., Lindhout, D., Cole, W.G., Henn, W. and Knoll, J.H. (1997) Mutations involving the transcription factor CBFA1 cause cleidocranial dysplasia. *Cell*, **89**, 773–779.
6. Brown, S.A., Warburton, D., Brown, L.Y., Yu, C.Y., Roeder, E.R., Stengel-Rutkowski, S., Hennekam, R.C.M. and Muenke, M. (1998) Holoprosencephaly due to mutations in ZIC2, a homologue of *Drosophila* odd-paired. *Nat. Genet.*, **20**, 180–183.
7. Goodman, F.R., Bacchelli, C., Brady, A.F., Brueton, L.A., Fryns, J.P., Mortlock, D.P., Innis, J.W., Holmes, L.B., Donnenfeld, A.E. and Feingold, M. (2000) Novel HOXA13 mutations and the phenotypic spectrum of hand-foot-genital syndrome. *Am. J. Hum. Genet.*, **67**, 197–202.
8. Crisponi, L., Deiana, M., Loi, A., Chiappe, F., Uda, M., Amati, P., Bisceglia, L., Zelante, L., Nagaraja, R. and Porcu, S. (2001) The putative forkhead transcription factor FOXL2 is mutated in blepharophimosis/ptosis/epicanthus inversus syndrome. *Nat. Genet.*, **27**, 159–166.
9. Forood, B., Perez-Paya, E., Houghten, R.A. and Blondelle, S.E. (1995) Formation of an extremely stable polyalanine beta-sheet macromolecule. *Biochem. Biophys. Res. Commun.*, **211**, 7–13.
10. Shanmugam, V., Dion, P., Rochefort, D., Laganiere, J., Brais, B. and Rouleau, G.A. (2000) PABP2 polyalanine tract expansion causes intranuclear inclusions in oculopharyngeal muscular dystrophy. *Ann. Neurol.*, **48**, 798–802.
11. Rankin, J., Wyttenbach, A. and Rubinsztein, D.C. (2000) Intracellular green fluorescent protein-polyalanine aggregates are associated with cell death. *Biochem J.*, **348**, 15–19.

12. Fan, X., Dion, P., Laganiere, J., Brais, B. and Rouleau, G. (2001) Oligomerization of polyalanine expanded PABPN1 facilitates nuclear protein aggregation that is associated with cell death. *Hum. Mol. Genet.*, **10**, 2341–2351.
13. Calado, A., Tome, F.M.S., Brais, B., Rouleau, G.A., Kuhn, U., Wahle, E. and Carmo-Fonseca, M. (2000) Nuclear inclusions in oculopharyngeal muscular dystrophy consist of poly (A) binding protein 2 aggregates which sequester poly(A) RNA. *Hum. Mol. Genet.*, **9**, 2321–2328.
14. Becher, M.W., Kotzuk, J.A., Davis, L.E. and Bear, D.G. (2000) Intranuclear inclusions in oculopharyngeal muscular dystrophy contain poly(A) binding protein 2. *Ann. Neurol.*, **48**, 812–815.
15. Uyama, E., Tsukahara, T., Goto, K., Kurano, Y., Ogawa, M., Kim, Y.J., Uchino, M. and Arahata, K. (2000) Nuclear accumulation of expanded PABP2 gene product in oculopharyngeal muscular dystrophy. *Muscle Nerve*, **23**, 1549–1554.
16. Fan, X. and Rouleau, G. (2003) Progress in understanding the pathogenesis of oculopharyngeal muscular dystrophy. *Can. J. Neurol. Sci.*, **30**, 8–14.
17. Tome, F.M. and Fardeau, M. (1980) Nuclear inclusions in oculopharyngeal dystrophy. *Acta Neuropathol. (Berl.)*, **49**, 85–87.
18. Cummings, C.J., Mancini, M.A., Antalffy, B., DeFranco, D.B., Orr, H.T. and Zoghbi, H.Y. (1998) Chaperone suppression of aggregation and altered subcellular proteasome localization imply protein misfolding in SCA1. *Nat. Genet.*, **19**, 148–154.
19. Wyttenbach, A., Carmichael, J., Swartz, J., Furlong, R.A., Narain, Y., Rankin, J. and Rubinsztein, D.C. (2000) Effects of heat shock protein 40 (HDJ-2) and proteasome inhibition on protein aggregation in cellular models of Huntington's disease. *Proc. Natl Acad. Sci. USA*, **97**, 2898–2903.
20. Chai, Y., Koppenhafer, S.L., Shoesmith, S.J., Perez, M.K. and Paulson, H.L. (1999) Evidence for proteasome involvement in polyglutamine disease: localization to nuclear inclusions in SCA3/MJD and suppression of polyglutamine aggregation *in vitro*. *Hum. Mol. Genet.*, **8**, 673–682.
21. Stenoien, D.L., Cummings, C.J., Adams, H.P., Mancini, M.G., Patel, K., DeMartino, G.N., Marcelli, M., Weigel, N.L. and Mancini, M.A. (1999) Polyglutamine-expanded androgen receptors form aggregates that sequester heat shock proteins, proteasome components and SRC-1 and are suppressed by the HDJ-2 chaperone. *Hum. Mol. Genet.*, **8**, 731–741.
22. Seufert,W. and Jentsch, S. (1990) Ubiquitin-conjugating enzymes UBC4 and UBC5 mediate selective degradation of short-lived and abnormal proteins. *EMBO J.*, **9**, 543–550.
23. Sommer, T. and Seufert, W. (1992) Genetic analysis of ubiquitin-dependent protein degradation. *Experientia*, **48**, 172–178.
24. Watt, R. and Piper, P.W. (1997) UB14, the polyubiquitin gene of *Saccharomyces cerevisiae*, is a heat shock gene that is also subject to catabolite derepression control. *Mol. Gen. Genet.*, **253**, 439–447.
25. Hershko, A. and Ciechanover, A. (1998) The ubiquitin system. *A. Rev. Biochem.*, **67**, 425–479.
26. Schwartz, A.L. and Ciechanover, A. (1999) The ubiquitin–proteasome pathway and pathogenesis of human diseases. *A. Rev. Med.*, **50**, 57–74.
27. Ciechanover, A., Orian, A. and Schwartz, A.L. (2000) Ubiquitin-mediated proteolysis: biological regulation via destruction. *Bioessays*, **22**, 442–451.
28. Yamamoto, A., Lucas, J.J. and Hen, R. (2000) Reversal of neuropathology and motor dysfunction in a conditional model of Huntington's disease. *Cell*, **101**, 57–66.
29. Wahle, E. (1991) A novel poly (A)-binding protein acts as a specificity factor in the second phase of messenger RNA polyadenylation. *Cell*, **66**, 759–768.
30. Bao, Y.P., Cook, L.J., O'Donovan, D., Uyama, E. and Rubinsztein, D.C. (2002) Mammalian, yeast, bacterial, and chemical chaperones reduce aggregate formation and death in a cell model of oculopharyngeal muscular dystrophy. *J. Biol. Chem.*, **277**, 12263–12269.
31. Goellner, G.M. and Rechsteiner, M. (2003) Are Huntington's and polyglutamine-based ataxias proteasome storage diseases? *Int. J. Biochem. Cell Biol.*, **35**, 562–571.
32. Sakahira, H., Breuer, P., Hayer-Hartl, M.K. and Hartl, F.U. (2002) Molecular chaperones as modulators of polyglutamine protein aggregation and toxicity. *Proc. Natl Acad. Sci. USA* early edition, **99**, 1–7.
33. Keller, R.W., Kuhun, U., Aragon, M., Bornikova, L., Wahle, E. and Bear, D.G. (2000) The nuclear poly (A) binding protein, PABP2, forms an oligomeric particle covering the length of the poly(A) tail. *J. Mol. Biol.*, **297**, 569–583.
34. Sittler, A., Lurz, R., Lueder, G., Priller, J., Lehrach, H., Hayer-Hartl, M.K., Hartl, F.U. and Wanker, E.E. (2001) Geldanamycin activates a heat shock response and inhibits huntingtin aggregation in a cell culture model of Huntington's disease. *Hum. Mol. Genet.*, **10**, 1307–1315.
35. Cummings, C.J., Sun, Y., Opal, P., Antalffy, B., Mestril, R., Orr, H.T., Dillmann, W.H. and Zoghbi, H.Y. (2001) Over-expression of inducible HSP70 chaperone suppresses neuropathology and improves motor function in SCA1 mice. *Hum. Mol. Genet.*, **10**, 1511–1518.
36. Fernandez-Funez, P., Nino-Rosales, M.L., de Gouyon, B., She, W.C., Luchak, J.M., Martinez, P., Turiegano, E., Benito, J., Capovilla, M., Skinner, P.J. *et al.* (2000) Identification of genes that modify ataxin-1-induced neurodegeneration. *Nature*, **408**, 101–106.
37. Kazemi-Esfarjani, P. and Benzer, S. (2000) Genetic suppression of polyglutamine toxicity in *Drosophila*. *Science*, **287**, 1837–1840.
38. Warrick, J.M., Chan, H.Y., Gray-Board, G.L., Chai, Y., Paulson, H.L. and Bonini, N.M. (1999) Suppression of polyglutamine-mediated neurodegeneration in *Drosophila* by the molecular chaperone HSP70. *Nat. Genet.*, **23**, 425–428.
39. Chai, Y., Koppenhafer, S.L., Bonini, N.M. and Paulson, H.L. (1999b) Analysis of the role of heat shock protein (Hsp) molecular chaperones in polyglutamine disease. *J. Neurosci.*, **19**, 10338–10347.
40. Chan, H.Y.E., Warrick, J.M., Gray-Board, G.L., Paulson, H.L. and Bonini, N.M. (2000) Mechanisms of chaperone suppression of polyglutamine disease: selectivity, synergy and modulation of protein solubility in *Drosophila*. *Hum. Mol. Genet.*, **9**, 2811–2820.
41. Sherman, M.Y. and Goldberg, A.L. (2001) Cellular defenses against unfolded proteins: a cell biologist thinks about neurodegenerative diseases. *Neuron*, **29**, 15–32.
42. Mogk, A., Mayer, M.P. and Deuerling, E. (2002) Mechanisms of protein folding: molecular chaperones and their application in biotechnology. *Chembiochemistry*, **3**, 807–814.
43. Muchowski, P.J., Schaffar, G., Sittler, A., Wanker, E.E., Hayer-Hartl, M.K. and Hartl, F.U. (2000) Hsp70 and Hsp40 chaperones can inhibit self-assembly of polyglutamine proteins into amyloid-like fibrils. *Proc. Natl Acad. Sci. USA*, **97**, 7841–7846.
44. Bailey, C.K., Andriola, I.F.M., Kampinga, H.H. and Merry, D.E. (2002) Molecular chaperones enhance the degradation of expanded polyglutamine repeat androgen receptor in a cellular model of spinal and bulbar muscular atrophy. *Hum. Mol. Genet.*, **11**, 515–523.
45. Bence, N.F., Sampat, R.M. and Kopito, R.R. (2001) Impairment of the ubiquitin–proteasome system by protein aggregation. *Science*, **292**, 1467–1468.
46. Verhoef, L.G., Lindsten, K., Masucci, M.G. and Dantuma, N.P. (2002) Aggregate formation inhibits proteasomal degradation of polyglutamine proteins. *Hum. Mol. Genet.*, **11**, 2689–2700.
47. Hattori, H., Kaneda, T., Lokeshwar, B., Laszlo, A. and Ohtsuka, K. (1993) A stress-inducible 40 kDa protein (hsp40): purification by modified two-dimensional gel electrophoresis and co-localization with hsc70 (p73) in heat-shocked HeLa cells. *J. Cell Sci.*, **104**, 629–638.
48. Welch, W.J. and Feramisco, J.R. (1984) Nuclear and nucleolar localization of the 72,000-dalton heat shock protein in heat-shocked mammalian cells. *Biol. Chem.*, **259**, 4501–4513.
49. Kim, S., Nollen, E.A., Kitagawa, K., Bindokas, V.P. and Morimoto, R.I. (2002) Polyglutamine protein aggregates are dynamic. *Nat. Cell Biol.*, **10**, 826–831.
50. Ravikumar, B., Duden, R. and Rubinsztein, D. (2002) Aggregate-prone proteins with polyglutamine and polyalanine expansions are degraded by autophagy. *Hum. Mol. Genet.*, **11**, 1107–1117.
51. Rattan, S.I. and Derventzi, A. (1991) Altered cellular responsiveness during ageing. *Bioessays*, **13**, 601–606.
52. Heydari, A.R., Takahashi, R., Gutsmann, A., You, S. and Richardson, A. (1994) Hsp70 and aging. *Experientia*, **50**, 1092–1098.
53. Bukau, B. and Horwich, A.L. (1998) The Hsp70 and Hsp60 chaperon machines. *Cell*, **92**, 351–366.
54. Kobayashi, Y., Kume, A., Li, M., Doyu, M., Hata, M., Ohtsuka, K. and Sobue, G. (2000) Chaperones Hsp70 and Hsp40 suppress aggregate formation and apoptosis in cultured neuronal cells expressing truncated androgen receptor protein with expanded polyglutamine tract. *J. Biol. Chem.*, **275**, 8772–8778.
55. Jana, N.R., Tanaka, M., Wang, G. and Nukina, N. (2000) Polyglutamine length-dependent interaction of Hsp40 and Hsp70 family chaperones with truncated N-terminal huntingtin: their role in suppression of aggregation and cellular toxicity. *Hum. Mol. Genet.*, **9**, 2009–2018.

56. Adachi, H., Katsuno, M., Minamiyama, M., Sang, C., Pagoulatos, G., Angelidis, C., Kusakabe, M., Yoshiki, A., Kobayashi, Y., Doyu, M. and Sobue, G. (2003) Heat shock protein 70 chaperone overexpression ameliorates phenotypes of the spinal and bulbar muscular atrophy transgenic mouse model by reducing nuclear localized mutant antrogen receptor protein. *J. Neurosci.*, **23**, 2203–2211.
57. Dou, F., Netzer, W.J., Tanemura, K, Li, F., Hartl, U., Takashima, A., Gouras, G., Greengard, P. and Xu, H. (2003) Chaperones increase association of tau protein with microtubules. *Proc. Natl Acad. Sci. USA*, **100**, 721–726.
58. Tsai, Y.C., Fishman, P., Thakor, N.V. and Oyler, G.A. (2003) Parkin facilitates the elimination of expanded polyglutamine proteins and leads to preservation of proteasome function. *J. Biol. Chem.*, **278**, 22044–22055.
59. Scherzinger, E., Lurz, R., Turmaine, M., Mangiarini, L., Hollenbach, B., Hasenbank, R., Bates, G.P., Davies, S.W., Lehrach, H. and Wanker, E.E. (1997) Huntingtin-encoded polyglutamine expansions form amyloid-like protein aggregates *in vitro* and *in vivo*. *Cell*, **90**, 549–558.
60. Wanker, E.E., Scherzinger, E., Heiser, V., Sittler, A., Eichkoff, H. and Lehrach, H. (1999) Membrane filter assay for detection of amyloid-like polyglutamine-containing protein aggregates. *Meth. Enzymol.*, **309**, 375–386.